Task 1.1

The mixing of the thrusts that result in the control forces and the control torque moments are given using matrix representation as follows:

$$\begin{bmatrix} T_c \\ L_c \\ M_c \\ N_c \end{bmatrix} = \underbrace{\begin{bmatrix} -1 & -1 & -1 & -1 \\ -\frac{b}{\sqrt{2}} & +\frac{b}{\sqrt{2}} & +\frac{b}{\sqrt{2}} & -\frac{b}{\sqrt{2}} \\ +\frac{b}{\sqrt{2}} & -\frac{b}{\sqrt{2}} & +\frac{b}{\sqrt{2}} & -\frac{b}{\sqrt{2}} \\ +\sigma & +\sigma & -\sigma & -\sigma \end{bmatrix}}_{\text{input matrix W}} \begin{bmatrix} T_1 \\ T_2 \\ T_3 \\ T_4 \end{bmatrix}$$

The control force is the sum of the individual torques with a direction opposite to the ones of the thrusts.

The torque moments are again a mix of the thrusts and are given by the following equations:

$$L_c = -(b/\sqrt{2})T_1 + (b/\sqrt{2})T_2 + (b/\sqrt{2})T_3 - (b/\sqrt{2})T_4$$

$$M_c = (b/\sqrt{2})T_1 - (b/\sqrt{2})T_2 + (b/\sqrt{2})T_3 - (b/\sqrt{2})T_4$$

$$N_c = +\sigma T_1 + \sigma T_2 - \sigma T_3 - \sigma T_4$$

The interesting observations to be made are related to the how these torque components are dependent on the thrusts from the propellers. Specifically, Lc has a positive value when the sum of T2 and T3 is bigger than the sum of T1 and T4, and negative otherwise.

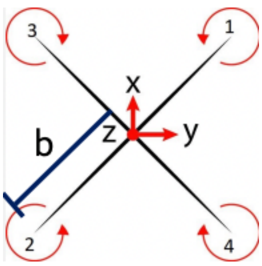

Lc thus shows the direction of rolling of the drone with respect to the x axis as shown in the image. Mc on the other hand shows the pitch of the drone, which is similar to Lc but shows the motion of the drone in the y axis.

To conclude, Nc is proportional to the constant σ which is a characteristic of the gas medium the drones propagates through. Nc dictates whether the drone moves clockwise or anticlockwise with respect to each center.

Task 1.2

Having a complex non-linear system is difficult to handle. There are many variables that affect the system and error can accumulate quickly. Given how our system is set and is controlled, many variables are fixed, which allows our system to become simpler and our non-linear equations can be replaced with much simpler linear ones that would produce enormous amounts of error if our system was not limited.

Task 1.3

As explained in the lab notes, there are 2 sampling rates present in our system. The first one is the Controller Sampling rate which is 250Hz and that is the frequency of propagation of signals in the FCU. The second one is the telemetry sample rate which is 100Hz which is used for logging purposes mostly and telemetry.

All the components used within a digital controller introduce an added path for electrical signals to propagate. The total optical path needed for the signals to propagate through our control system indicates the time needed for our system to produce a constant result. This time must be smaller than the sampling period so the controller sampling rate must be carefully picked to accommodate to that.

Task 2.1

Slide 3

When ignoring delays the linearised equations are the ones explained in the lab notes

The first equation is $\Delta\dot{\theta} = \Delta q$. The second equation is $J_\theta \Delta\dot{q} = \dot{M}_c + M_e$

A general form of the exogenous torque taken from slide 5 of the lab notes is:

$$M_e = -cq - k\theta$$

Where k is the stiffness coefficient which is related to gravity force and any offset of the Center of Mass(CoM) of the drone with respect to the shaft axis and c is the damping coefficient which is composed both by the aerodynamic damping and the bearings friction.

To conclude, the pitch axis dynamics can be rewritten using first order differential equations which is crucial to describe our control system:

$$\dot{\theta} = q$$

$$\dot{q} = -2\xi\omega_n q - \omega_n^2\theta + \mu M_c^d$$

ξ = damping ratio

ω_n= natural frequency

μ = input gain

M_c^d = desired pitch moment.

Task 2.2

Initial experiments with the drone had to do with the analysis of the system's parameters and how they relate to an introduction of torques. The drone is left to oscillate freely so that the oscillation period and the settling time is measured.

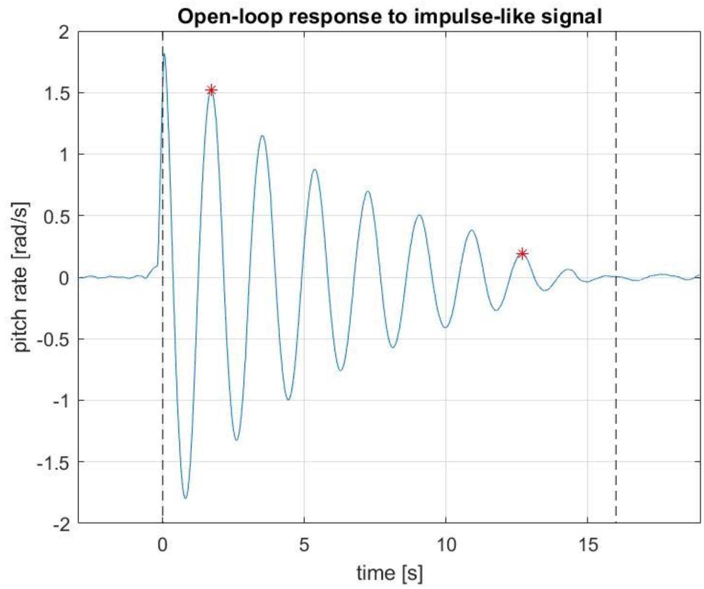

$$T_P = \frac{2\pi}{\omega_n\sqrt{1-\xi^2}} \approx \frac{2\pi}{\omega_n}$$

$$T_s \approx \frac{4.6}{\xi\omega_n}.$$

The period of the dumping was found to be T = 1.82s. The settling time was found to be Ts = 16s. From the above one can calculate the natural frequency of oscillation to be wn = 3.44 rad/s , and xi = 0.084.

Task 2.3

Proceeding with the experiment, we use a doublet excitation signal to measure the doublet response of the system that allows to measure the gain mu. This is done by finding the ratio of amplitudes of the response of the system with one that has a gain of 1.

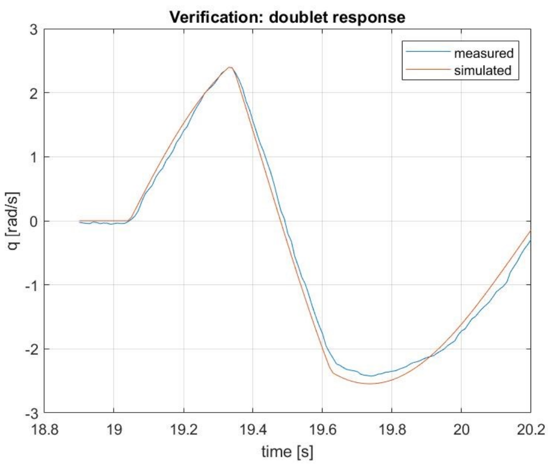

There are some deviations between the model and experiment. As the experimental configuration is using digital sensors to take measurements which means that there will be delay in changes to the system which are translated to more subtle and delayed changes to our response. The gain of the system was found to be mu = 358.5. Based on the sampling frequency, the delay seems to be about 2 samples.

Task 3.1

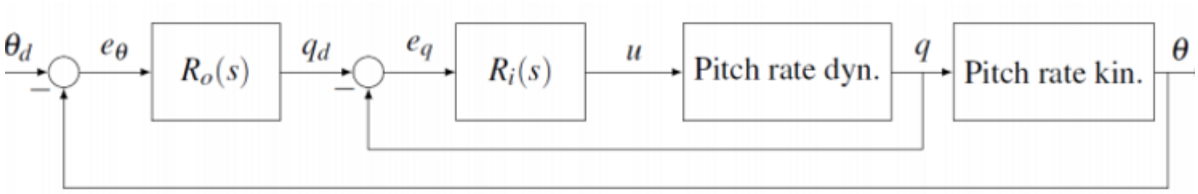

The angle control system is as follows. There are two loops in our system. The outer one is used to calculate the angle and the inner one is used to calculate the angular rate. The input of the control system is the desired attitude to the system. A PID controller is used to tune the desired angular rate that is the input of the inner loop. The inner loop again uses a PID controller to set the input to the pitch rate dynamics system. It is important that the inner loop of a control system has a higher bandwidth frequency than the outer loop so that it stabilises in value faster than the outer loop ensuring separation. Specifically, the inner loop has a bandwidth of approximately 30 rads/s while the outer loop is 10 rad/s. The above values ensure separation which is important for noise rejection in our system.

$$R_i(s) = K_p^i + \frac{K_i^i}{s} + K_d^i \frac{s}{\tau_f s + 1}$$

Task 3.2

As explained in the previous task, PID controllers are widely used in our system. A PID controller stabilises the value of the angular rate close to a desired value that tunes the PID controller of the attitude system. PID controllers use the error between a desired and an actual value of a quantity to tune the system to stabilise to an equilibrium close to the desired value. Having two dependent loops with their respective PID controller ensures a robust pipeline for controlling two system parameters.

Task 3.3

The history plot of pitch rate control is shown below:

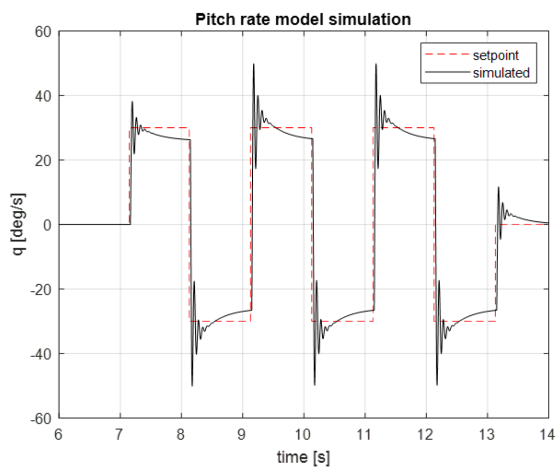

The graph shows an average agreement with the desired setpoint. The differences occur in the discontinuities of the rectangle wave. This is because our PID parameters are not tuned ideally so that the system can stabilise faster to the changes.

Task 3.4

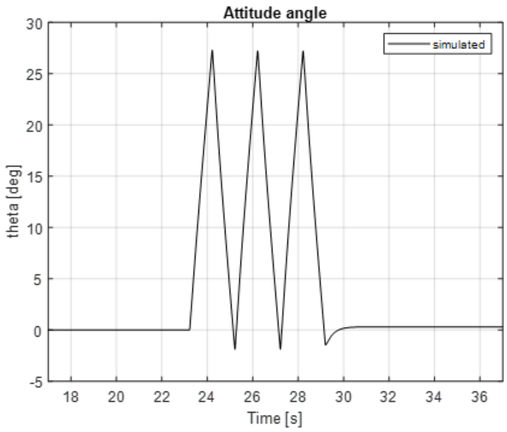

Unfortunately, the simulated attitude angles can not be directly compared with experiment, but from personal investigation, the expectation is a similar behaviour with small discrepancies due to errors in the conduction of the experiment.

Task 3.5

The complete table of our measurements is shown below:

Loop shaping results for different parameters are shown below:

	Kp	Ki	Kd	ω_c^d (rad/s)	τ1	τ2	$\bar{\mu}$	ω_c(rad/s)	ω_m(deg)
Mid-BW	0.0854	0.251	$5.4*10^{-4}$	30	0.33	0.0167	90	32.6	57.8
Low-BW	0.029	0.0279	0.0011	10	1	0.05	10	11.5	95.2
High-BW	0.1127	0.446	$2.68*10^{-4}$	40	0.25	0.0125	160	41.5	41.8

For reduced order, full order for both discrete and continuous systems, the results are shown below:

	ω_c^d (rad/s)	RCω_c(rad/s)	RCϕ_m(deg)	FCω_c(rad/s)	FCω_m(deg)	FDω_c(rad/s)	FDϕ_m(deg)
Mid-BW	30	32.6	57.8	33	58.5	33.5	57.7
Low-BW	10	11.5	95.2	12.7	98.7	12.8	98.6
High-BW	40	41.5	41.8	42.1	42	42.6	41.3

Reduced order systems seem to approximate desired corner frequencies better than Full order ones. PID controllers generally work well with systems that have reduced dynamics as they provide versatility in approximating simple relations. When the dynamics of the system get more complicated, a PID seems to be unable to allow the system to reach a close equilibrium to the desired value. When comparing Discrete with Continuous systems, one should consider all the useful information lost due to sampling. This error in measurements is translated in a less optimal parameter tuning.

The bode plot of the complementary sensitivity function of our system during our measurements is shown below:

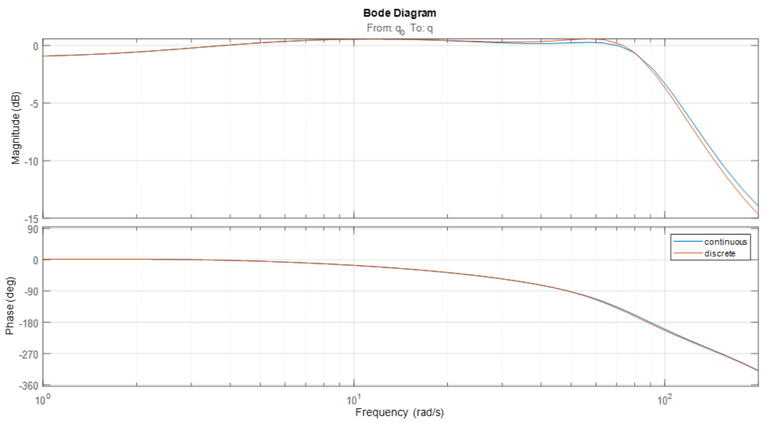

High frequency noise is reduced due to the complementary sensitivity function which is similar to a low pass filter. It is clearly visible that the discrete system has a lower corner frequency which is due to the finite resolution of its filter.

Task 3.6

For the case of 10 rads/s crossover frequency:

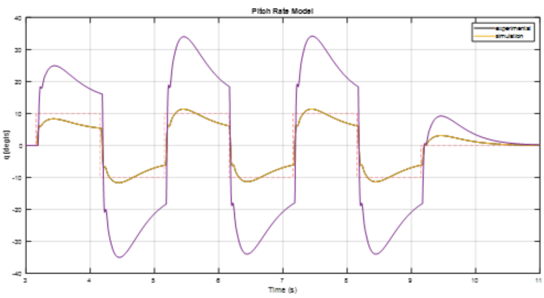

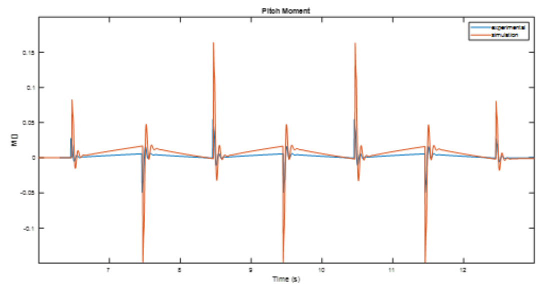

The system performs subpar in the case of a low bandwidth. The system is not allowed to react to changes to parameters fast enough to stabilize and that is why such a bad performance is observed. For the case of 30 rad/s crossover frequency:

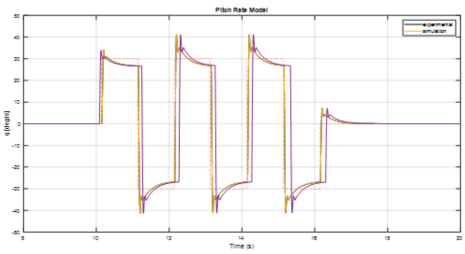

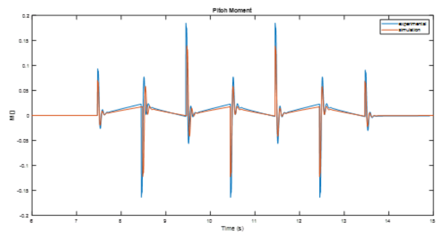

As the bandwidth of the system increases, a much more adequate response to changes is observed. The system rejects most of the disturbance introduced to it and it allows for adequate equilibria to be reached fast enough. For a higher bandwidth one should note that the system is affected highly by noise.

Task 4.1

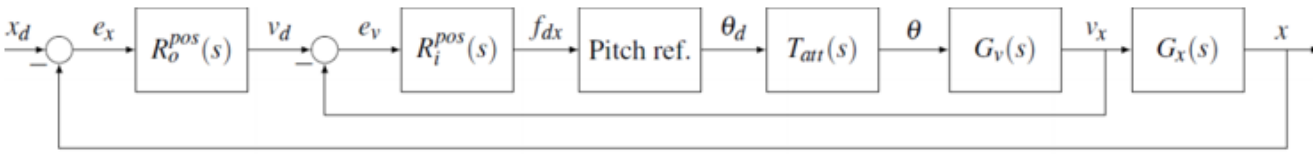

As taken from the lectures, this is the position dynamics control system. It extends from the previously investigated attitude control system which is now the inner loop of the system. The input to the system is the position that the control system needs to stabilize close to. A new P controller is introduced that approximates the velocity needed to achieve the desired position. The new schematic disregards the angular velocity inner loop investigated in previous tasks. This is because that loop has a wide bandwidth separation compared to the outer loop of the system which makes the apparent gain of the loop have a magnitude of 1. From the lectures it is given that the bandwidth of the outer loop is approximately 1.5 rad/s which is immensely smaller than the angular rate loop and quite smaller than the inner attitude loop.

Task 4.2

Control Loop	Crossover Frequency	Phase Margin	Complementary sensitivity Bandwidth
Angular Rate	33.5	57.7	95.82
Attitude	11.7	71.4	19.55
Velocity	4.24	68.8	6.87
Position	1.49	70.8	2.39

From the table shown above it is clearly visible that our control system meets the requirements posed to it. The outer loop indeed has an approximate 1.5 rad/s crossover frequency, the attitude is close to 10 rad/s and the angular rate is close to 30 as the desired values for our system. This can be attributed to simplifying our system and having limited variability in our experimental setup. For the Phase Margin as well as the Complementary sensitivity Bandwidth the same comments apply as they are close to the desired values.

Task 4.3

The position controller for a low bandwidth configuration is shown below:

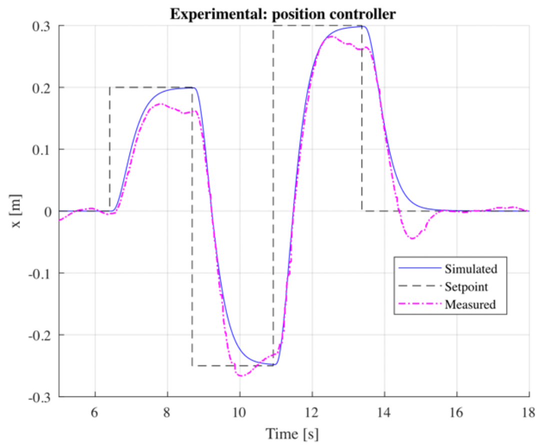

As it can be seen, the experimental and simulated values closely match with some discrepancies near the peaks which can be attributed to factors not taken into account by our model.

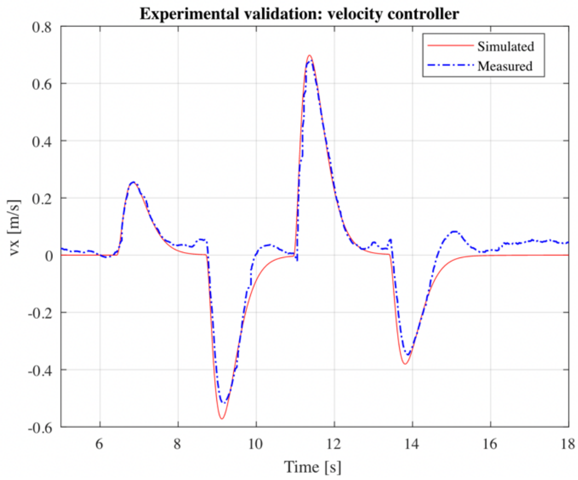

As we investigate the inner loops, a closer match between theory and experiment is observed. The common discrepancies still occur at abrupt changes but the system adapts to changes quickly.

Lastly for the attitude control system:

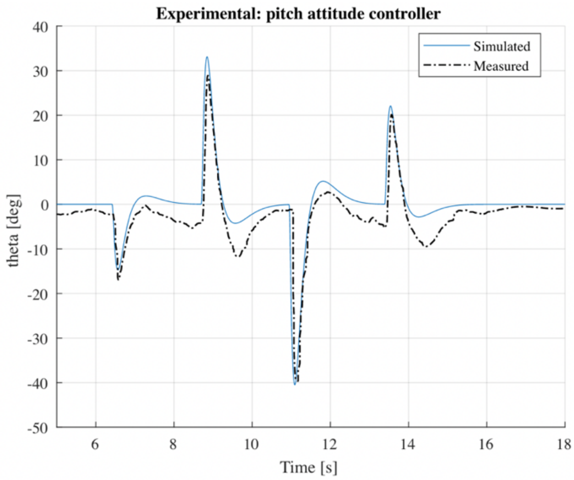

It can be observed that still the theory closely matches to experiment. There are some discrepancies that are greater than in the control system of the velocity. Generally controlling the angle of a system is a more difficult task as it has to do with more complex physics than controlling the linear velocity of the same system. This is even better explained by observing how the biggest discrepancies are at small changes to the angle. Our control system is really good at adapting to sudden changes but has limited resolution when it comes to small changes to our system.